

Title: Microfluidic flow cytometer for quantifying photobleaching of fluorescent proteins in cells

Authors: Jennifer L. Lubbeck^{1,2}, Kevin M. Dean¹, Hairong Ma^{1,2}, Amy E. Palmer¹, Ralph Jimenez^{1,2}

1 – Department of Chemistry & Biochemistry, University of Colorado Boulder, USA. 80309

2 – JILA, University of Colorado Boulder and National Institute of Standards and Technology, USA. 80309

Supporting Methods

Abstract

Here we present additional photophysical information on mOrange2, mCherry, TagRFP, and TagRFP-T including *in vitro* studies to determine the percent fluorescence recovery after photobleaching, photostabilities, and lifetimes. Furthermore, additional experimental details regarding *in vitro* analysis of the proteins, theoretical calculations and experimental setup are provided. Lastly, cytometry intensity calibration plots using commercially available fluorescent polystyrene beads are presented.

***In Vitro* Analysis**

Details regarding protein sample preparation for *in vitro* analysis has been reported previously¹.

Additional Information on Theoretical calculations

The intensity function of a radially symmetrical Gaussian beam may be written as

$$B[x, y, z] = \frac{2P}{\pi w^2[z]} \exp\left(-\frac{2(x^2 + y^2)}{w^2[z]}\right)$$

Where P is the total power of the beam and w[z] is the beam radius where the intensity drops to 1/e² of its peak value. The evolution of the Gaussian beam along the propagation direction, defined as the z axis here, is written as follows

$$w_i[z] = w_0 \sqrt{1 + \frac{z^2}{z_{Ri}^2}}$$

Where $z_R = \pi w_0^2 / \lambda$ is known as the Rayleigh range, at $z=z_R$ the radius of beam is $\sqrt{2}$ times larger than its waist value w_0 , or the beam area doubles.

For a Gaussian beam propagating through a cascade of optical elements in space, its wave function is modified by the optical elements (e.g. lenses) it passes through. Due to the unique transform characteristics of the Gaussian beam, its propagation can be treated analogous to geometric optics following a general ABCD matrix method, by defining a complex radius of curvature,

$$\frac{1}{\tilde{q}} = \frac{1}{R_z} - i \frac{\lambda}{\pi w^2[z]}$$

where R_z is the radius of curvature of the wave at position z .

In a case of astigmatic transformation, for example, the propagation of a Gaussian beam through a cylindrical lens, the evolution of the beam in the x and y directions differ and the evolution in each orthogonal direction can be treated independently.

In our experiment, a Gaussian beam from the laser first passes through a cylindrical lens ($f_y=150$ mm), then is focused by an objective lens ($20\times$, $NA=0.45$) onto the sample. The sample is placed at the x -axis focal point of the objective lens, where the beam has passed the y -axis focal point and is therefore expanded across the microfluidics channel. We first deduced the analytical propagation equation of the Gaussian beam in this astigmatic optical system, then calculated the emission signal intensity of the fluorescent cells as they traverse through the beams. Here for simplicity we treated the objective lens as a simple lens with a specified focal length of 9 mm, as it is neither practical nor necessary to trace the beam propagation through each one of the dozens or more individual optical elements in a modern objective lens. In the x direction in which the cylindrical lens does not focus, the beam transfer matrix may be written as

$$M_x = \begin{bmatrix} 1 - \frac{z_0}{f_{obj}} & z_0 \\ -\frac{1}{f_{obj}} & 1 \end{bmatrix}$$

where z_0 is the distance between the objective lens and the sample, which is placed at the x-axis waist position, and f_{obj} is the focal length of the objective lens. The transfer matrix in the y direction can be calculated in a similar way, except that the cylindrical lens needs to be included in the transfer matrix.

The deduced analytical form of the Gaussian beam after the objective can be written as

$$B[x, y, z] = \frac{2P}{\pi w_x[z] w_y[z]} \exp\left(-\left(\frac{2x^2}{w_x^2[z]} + \frac{2y^2}{w_y^2[z]}\right)\right)$$

where $w_x[z]$ and $w_y[z]$ follow the similar definitions as $w[z]$. If we define the center of the objective lens as the z-axis origin where $z=0$, $w_x[z]$ and $w_y[z]$ may be written as

$$w_i[z] = w_{0i} \sqrt{1 + \frac{(z - z_{0i})^2}{z_{Ri}^2}}$$

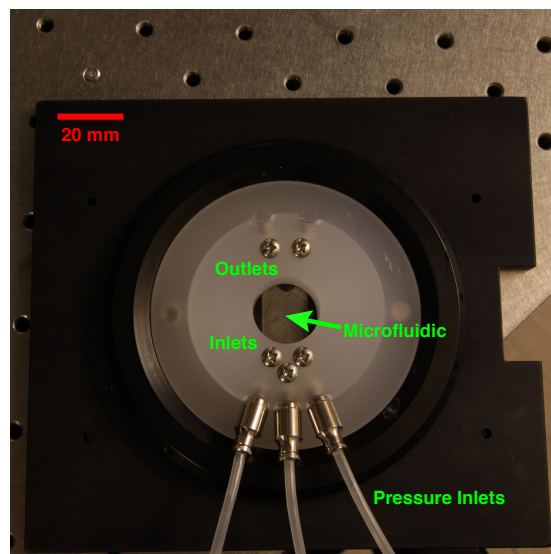
Where i denotes x or y, and w_{0i} specifies the beam waist in the i direction.

Additional Fluorescence Activated Cell Sorting (FACS) Details:

Two days after the retroviral transduction of HeLa suspension cells, FACS was used to enrich the population of successfully infected cells (RFP fluorescence positive). Fluorescent cells were enriched using a commercial flow-cytometer at a concentration of approximately 10^6 cells/mL in Ca^{2+} and Mg^{2+} free HHBSS, pH=7.4. Excitation was performed with a 568 nm krypton laser, forward scatter was used to trigger acquisition, and the fluorescence emission was separated from the excitation scatter by use of a 630/30 band-pass filter. The PMT was set at 450 volts, and forward scatter, side-scatter, and fluorescence were all operated in logarithmic modes. The flow-cytometer was maintained at around 2,000 events/second. Sufficient optical alignment was confirmed by a narrow (1.3 %) CV using Beckman Coulter Flow-Check Fluorospheres (part number: 6605359, diameter = 10 μ m). Uninfected, and thus non-fluorescent, HeLa suspension cells were used to set the threshold (or “gate”) and so the sort attempted to select all cells with fluorescence greater than cellular autofluorescence. FACS was only performed initially for each individual cell-line, and G418 (working concentration of 100 mg/mL) was applied to select against potential loss of retroviral gene insertion. The

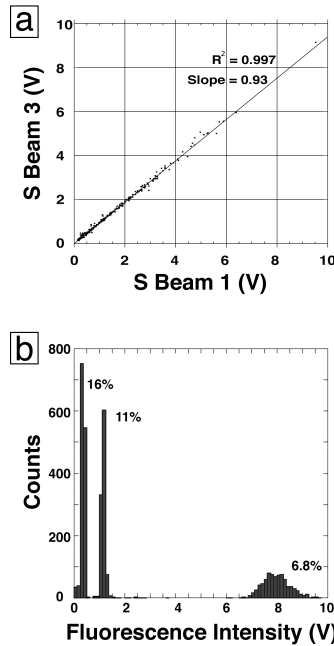
fluorescence observed for virally transduced cells varied from cell-line to cell line in the following manner:

Protein Expressed in Cells	Vector	Fluorescence CV
TagRFP-T	pCLNCX	131.52%
TagRFP	pCLNCX	158.26%
mCherry	pCL-Tet-On	250.16%
mOrange2	pCL-Tet-On	145.77%

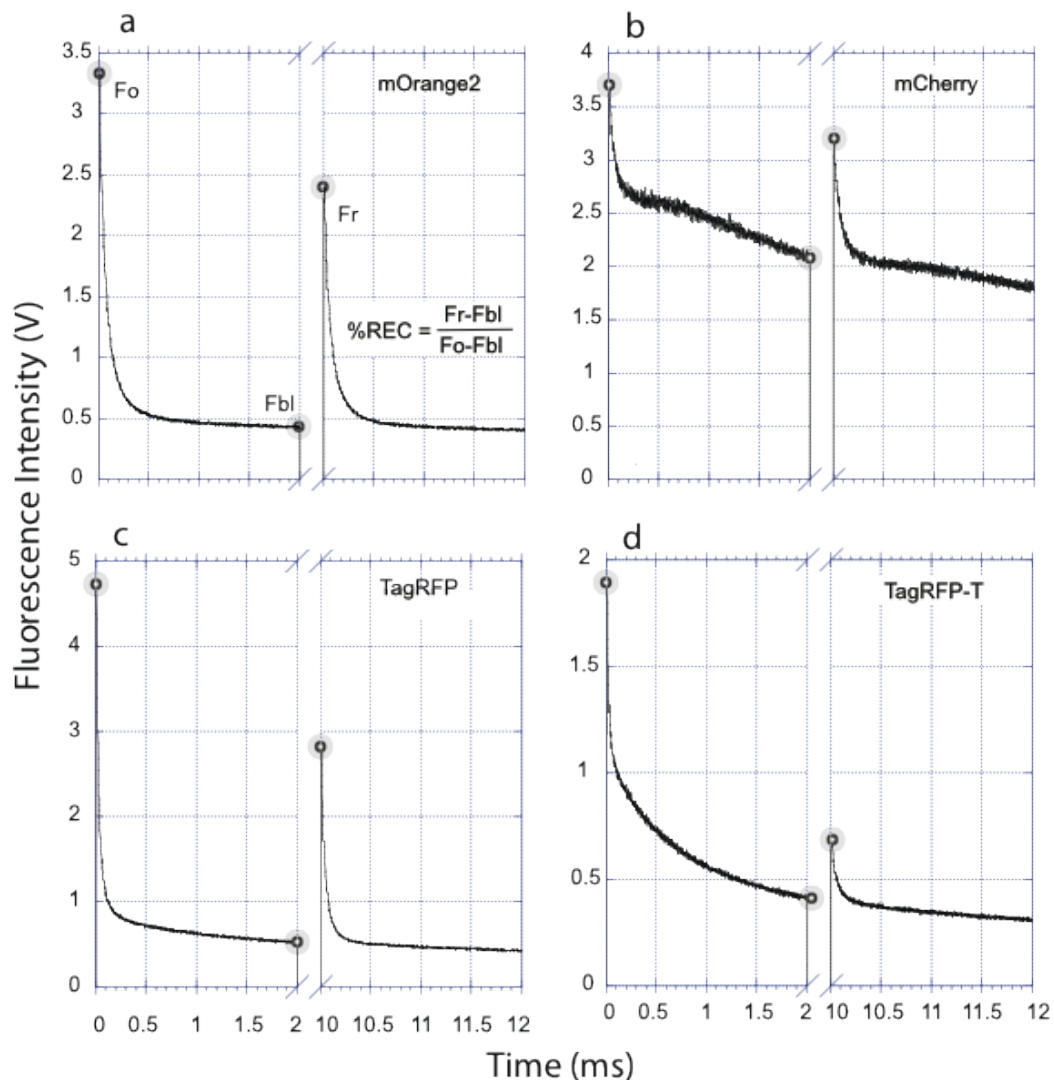


Supporting Figure S-1: Microfluidic holder.

Instrument Validation and Theoretical Considerations



Supporting Figure S-2: Commercially available intensity calibration beads (Invitrogen LinearFlow Deep Red Flow Cytometry Intensity Calibration Kit), suspended in a density matched 20% (v/v) glycerol in water solution) were used to characterize the microfluidic cytometer. **(a)** Using a mixture of beads with different fluorescence intensities, the correlation between the two probe beams was determined to be linear. The data collected in this run resulted in a slope of 0.93 with a CV of 7%. **(b)** With a single excitation beam (10 kW/cm^2), mixtures of polystyrene beads with three different fluorophore densities were resolved and yielded fluorescence intensity coefficients of variation (CV, listed as % in the above figure) similar (less than 10% different on average) to those measured individually on a FACS in a linear fluorescence mode (from left to right: 12.1%, 11.3%, and 7.8%). Additionally, our microfluidic platform detected all but the most-weakly fluorescent beads, those which have intensities comparable to cellular autofluorescence on a standard flow cytometer. Furthermore, the flexibility of our microfluidic platform permitted accurate measurement of fluorescence intensities spanning three orders of magnitude (0.1-10.0 V). Our signal to noise was limited by the noise-floor of our trans-impedance amplifier and saturation of our PMT or analog-to-digital conversion hardware, enabling the user to tune the cytometer for maximum utility within a specific range of fluorescence intensities.



Supporting Figure S-3: Photobleaching measurements were conducted with a 2 ms, 25 kW/cm² pulse of illumination from a 532 nm CW laser. The cells were then kept in the dark for 8 ms allowing for fluorescence recovery before the next 2 ms pulse. This duty cycle was designed to resemble cytometry experimental parameters. However, due to experimental limitations, the intensity was reduced to an eighth of the cytometry bleach-beam **(a)** mOrange2 fluorescence recovery of $80 \pm 5\%$ (n=3). **(b)** mCherry fluorescence recovery of $92 \pm 6\%$ (n=3). **(c)** TagRFP fluorescence recovery of $76 \pm 7\%$ (n=3). **(d)** TagRFP-T fluorescence recovery of $58 \pm 18\%$ (n=3).

Supporting Table S-1: Photophysical properties for the four RFPs studied here.

Reported photostabilities are from Shaner *et al.*². Experimental details for the

RFP	Ex/Em Max (nm)	Abs. Cross-Section @ 532 nm. (cm ²)	Quantum Yield	Chromophore	Reported Photostability ² t _{1/2} (s)
mOrange2	550/563	1.36×10 ⁻¹⁶	0.55 ± 0.04	Tricylic ³	2,900
mCherry	586/609	1.45×10 ⁻¹⁶	0.16 ± 0.02	Cis ³	1,800
TagRFP	554/579	2.55×10 ⁻¹⁶	0.48 ± 0.04	Trans	550
TagRFP-T	555/580	2.93×10 ⁻¹⁶	0.47 ± 0.08	Trans	6,900

measurement of these photophysical properties can be found in previous work¹.

RFP	Percent Recovery 8 ms	Percent Recovery 1s	Percent Recovery 10s	ANOVA P-Value
mOrange2	70 ± 3 (n=3)	75 ± 2 (n=3)	72 ± 2 (n=2)	0.12
mCherry	73 ± 6 (n=2)	74 ± 7 (n=3)	81 ± 6 (n=2)	0.49
TagRFP	54 ± 1 (n=3)	62 ± 7 (n=3)	63 ± 7 (n=2)	0.14
TagRFP-T	20 ± 4 (n=3)	32 ± 5 (n=3)	26 ± 5 (n=2)	0.059

Supporting Table S-2: Percent recoveries ± the standard deviation for the four

RFPs after a 2 ms, 100 kW/cm² pulse of illumination from a 532 nm CW laser followed by either 8 ms, 1 s, and 10 s in the dark prior to the next 2 ms pulse. Experimental details are reported in previous work¹.

Bibliography:

1. Dean, K. M.; Lubbeck, J. L.; Binder, J. K.; Schwall, L. R.; Jimenez, R.; Palmer, A. E., Analysis of Red-Fluorescent Proteins Provides Insight into Dark-State Conversion and Photodegradation. *Biophys J* **2011**, *101* (4), 961-969.
2. Shaner, N. C.; Lin, M. Z.; McKeown, M. R.; Steinbach, P. A.; Hazelwood, K. L.; Davidson, M. W.; Tsien, R. Y., Improving the photostability of bright monomeric orange and red fluorescent proteins. *Nature Methods* **2008**, *5* (6), 545-551.
3. Shu, X.; Shaner, N. C.; Yarbrough, C. A.; Tsien, R. Y.; Remington, S. J., Novel chromophores and buried charges control color in mFruits. *Biochemistry-US* **2006**, *45* (32), 9639-47.